Offset-free all-fiber frequency comb with an acousto-optic modulator and two *f*–2*f* interferometers

OPEN ACCESS
Applied Physics Express **10**, 072501 (2017)
https://doi.org/10.7567/APEX.10.072501

Offset-free all-fiber frequency comb with an acousto-optic modulator and two *f*–2*f* interferometers

Keisuke Nakamura[1,2], Sho Okubo[1,2], Malte Schramm[1,2,3], Ken Kashiwagi[1,2], and Hajime Inaba[1,2*]

[1]*National Metrology Institute of Japan (NMIJ), National Institute of Advanced Industrial Science and Technology (AIST), Tsukuba, Ibaraki 305-8563, Japan*
[2]*JST, ERATO, MINOSHIMA Intelligent Optical Synthesizer Project, Tsukuba, Ibaraki 305-8563, Japan*
[3]*National Astronomical Observatory of Japan (NAOJ), Mitaka, Tokyo 181-8588, Japan*

*E-mail: h.inaba@aist.go.jp

Received April 24, 2017; accepted May 22, 2017; published online June 13, 2017

We demonstrate an erbium-based offset-free frequency comb using a fiber-coupled acousto-optic modulator. The comb has two *f*–2*f* interferometers; one is for carrier-envelope offset beat detection, and the other is for frequency-shifted offset beat detection. The frequency was shifted by placing the acousto-optic modulator in front of an amplifier and a highly nonlinear fiber for spectral broadening. We confirmed that the offset frequency was stabilized at zero and measured it by shifting it from zero. The Allan deviations of the measured offset frequency were 0.10 and 0.18 Hz with a 1 s averaging time and using feedback and feed-forward stabilization, respectively.

Noteworthy achievements stemming from the invention of the optical frequency comb are the detection of a carrier-envelope offset (CEO) beat and the stabilization of its frequency (f_{CEO}).[1] The stabilization of both f_{CEO} and the repetition frequency (f_{rep}) of the optical frequency comb enabled us to connect microwave and optical frequency regimes, and constituted innovative progress in frequency metrology. Intensive studies have led to the advancement of optical frequency comb technology. The comb spectrum has broadened from ultraviolet to mid-infrared,[2] and a relative frequency stability of 4×10^{-18} has been achieved for a 1 s averaging time with a 0.5 Hz measurement bandwidth.[3] Optical frequency combs are now being used not only for frequency metrology but also for length measurement,[4] gas analysis,[5] and even in astrophysics.[6]

Whereas f_{rep} can be phase-locked easily since it can be detected directly by a photodetector with a high signal-to-noise ratio (S/N), f_{CEO} stabilization is relatively difficult since the CEO beat detection and its phase-lock require an f–$2f$ interferometer and an actuator with a somewhat broad servo bandwidth. To enhance the functionality and usability of the combs, f_{CEO} controllability is important. Specifically, f_{CEO} stabilization at zero ($f_{CEO} = 0$) has been intensively studied, leading to an "offset-free comb". An offset-free comb consists of modes at integer-multiple frequencies of f_{rep} in the frequency domain, and it links microwaves to the optical frequency region as an ideal frequency divider and/or multiplier. In addition, it makes optical frequency measurements easier.

In general, f_{CEO} is stabilized using a phase-locked loop (PLL) that locks a signal phase to a reference signal phase. However, the PLL cannot be directly employed to stabilize f_{CEO} at zero because the PLL needs a carrier to detect the error signal. Some approaches have been reported for achieving an offset-free comb, namely, shifting f_{CEO} with an acousto-optic modulator (AOM),[7] using feed-forward controls to cancel f_{CEO} with an AOM,[8–10] employing carrier envelope phase controls via optical parametric processes[11] and difference frequency generation.[12,13] The last two methods need a rather complicated system with nonlinear processes that require very intense optical pulses.

In this study, we demonstrate an offset-free all-fiber frequency comb using a robust erbium-fiber-based frequency comb and a fiber-coupled AOM[14] with feedback and feed-forward controls for f_{CEO}. Furthermore, we evaluated the frequency stability of the stabilized f_{CEO} by using two f–$2f$ interferometers.

Figure 1(a) shows our experimental setup for the offset-free comb using feedback control. We used an erbium-doped fiber (EDF)-based mode-locked laser with a ring cavity configuration[15] as the comb source (oscillator). The mode-locking mechanism was nonlinear polarization rotation. The EDF in the oscillator was pumped by a 1480 nm laser diode. The center wavelength and the spectral bandwidth of the oscillator output beam were 1560 and 20 nm (full width at half maximum), respectively. The oscillator emitted a pulse train at a repetition rate of 100 MHz with an average power of 17.8 mW.

The output beam was divided into two branches with a 50 : 50 fiber coupler. Each output beam was optimally amplified[16] by an erbium-doped fiber amplifier (EDFA) and spectrally broadened through a highly nonlinear fiber (HNLF) to more than 1 octave. Each EDFA had a 3-m-long EDF that was bidirectionally pumped by two 980 nm laser diodes. Each CEO beat was detected through a common pass f–$2f$ interferometer.[17] The first branch (referred to as the "AOM branch") had a fiber-coupled AOM (Brimrose AMF-40-1550-2FP) positioned before the EDFA, while the second branch (referred to as the "raw branch") had no AOM. The operation frequency, substrate material, acoustic velocity in the substrate, and loss of the AOM were 40 ± 3 MHz, Ge/As/Se glass, 2500 m/s, and 5.4 dB, respectively. The delay time was approximately 2 μs as determined from the acoustic velocity. We observed a CEO beat with a signal-to-noise ratio (S/N) of 45 dB at a resolution bandwidth (RBW) of 300 kHz using the f–$2f$ interferometer in the raw branch. Its beat frequency was f_{CEO}. On the other hand, we observed a CEO beat with an S/N of 35 dB at a 300 kHz RBW using the interferometer in the AOM branch. The frequency was $f_{CEO/AOM} = |f_{CEO} - f_{AOM}|$ when the AOM was driven with f_{AOM}. The beat note was filtered and amplified at 40 MHz, and then a double-balanced mixer was used to detect the phase difference between the signal and a dual-channel function generator (FG) output (40 MHz). The output of the mixer was added to the injection current of the pump laser as the feedback signal via a loop filter for proportional integral

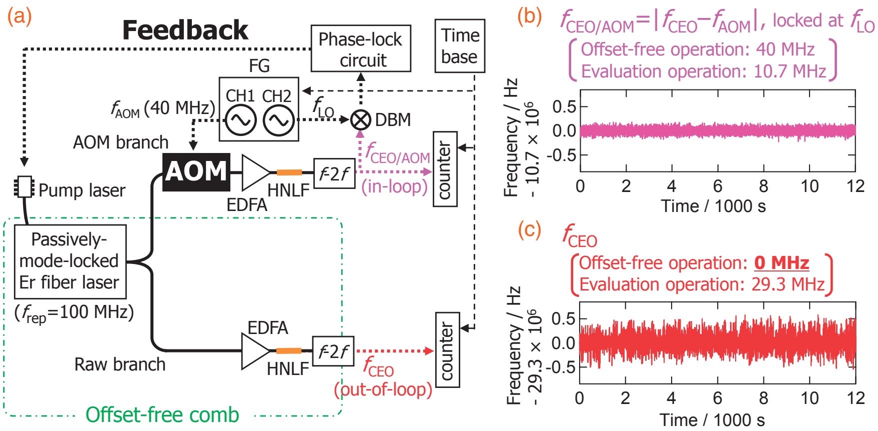

Fig. 1. (a) Experimental setup for "feedback" control. AOM: acousto-optic modulator, EDFA: erbium-doped fiber amplifier, HNLF: highly nonlinear fiber, f–2f: f–2f interferometer to detect CEO beat, DBM: double-balanced mixer, FG: dual-channel function generator, f_{AOM}: driving frequency of the AOM, f_{LO}: reference frequency for phase lock, $f_{CEO/AOM}$: CEO frequency observed at AOM branch, f_{CEO}: CEO frequency observed at raw branch. (b) $f_{CEO/AOM}$ and (c) f_{CEO} counted during evaluation operation.

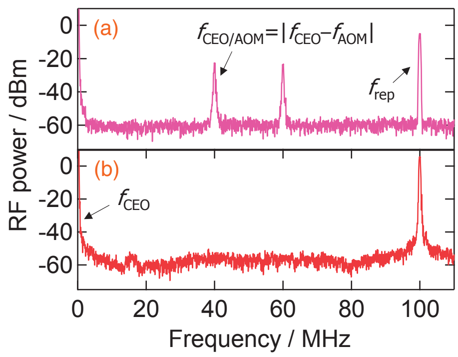

Fig. 2. RF CEO beat spectra in (a) AOM branch and (b) raw branch stabilized by "feedback" control. The resolution and video bandwidth were 300 and 30 kHz, respectively.

derivative (PID) control, which was described in our previous report[18] in detail.

The output from the raw branch is the offset-free comb when phase-locking $f_{CEO/AOM}$ to a reference frequency f_{LO}. f_{AOM} and f_{LO} are set equally at 40 MHz using the FG; this is referred to as "offset-free operation". Figures 2(a) and 2(b) show the CEO beat spectra observed in the AOM and the raw branch, respectively. In Fig. 2(b), the f_{CEO} signal is not visible since it overlaps zero and f_{rep}, and this strongly suggests that f_{CEO} is stabilized at zero.

To evaluate the performance of feedback control, we shifted f_{CEO} from zero to 29.3 MHz by shifting f_{LO} from 40 to 10.7 MHz without shifting f_{AOM}, and then counted f_{CEO} with a dead-time-free π-type frequency counter. We refer to the setting as an "evaluation operation". Figures 1(b) and 1(c) show $f_{CEO/AOM}$ (in-loop) and f_{CEO} (out-of-loop) with a 1 s averaging time. $f_{CEO/AOM}$ (in-loop) remained stable at 10.7 MHz with a fluctuation of less than 0.3 Hz, which indicates that feedback control worked properly and no cycle slips occurred. On the other hand, f_{CEO} (out-of-loop) remained at 29.3 MHz with a fluctuation of less than 0.6 Hz, which suggests that f_{CEO} was locked at zero during offset-free operation.

Figure 3(a) shows the experimental setup for the offset-free comb using feed-forward control. The only difference between this and feedback control is the electronics employed. The advantage of this configuration is that no active locking circuit is needed to stabilize f_{CEO}. In contrast to feedback control, the AOM branch output is the offset-free comb when feeding the free-running f_{CEO} signal (~40 MHz) to the AOM after filtering and amplifying it. We observed that $f_{CEO/AOM}$ was at zero with an RF spectrum analyzer as well as via the feedback experiment, as shown in Fig. 2(b).

To evaluate the performance of feed-forward control, we shifted $f_{CEO/AOM}$ from 0 to 29.3 MHz by shifting f_{CEO} from ~40 to ~10.7 MHz and mixing a 29.3 MHz signal with the f_{CEO} signal to generate an f_{AOM} signal of ~40 MHz. Figures 3(b) and 3(c) show $f_{CEO/AOM}$ and f_{CEO} counted with a 1 s averaging time. The counted $f_{CEO/AOM}$ remains at 29.3 MHz with a fluctuation of less than 0.9 Hz [Fig. 3(b)], which shows that the feed-forward control works properly, although the fluctuation is 1.5 times higher than that with feedback control [Fig. 1(b)]. Since f_{CEO} was free-running and drifted, we manually adjusted f_{AOM} to ~40 MHz by changing the pump power for the oscillator every ~500 s during the measurement to prevent f_{AOM} from exceeding the operation range of the AOM [Fig. 3(c)]. Long-term operation of feed-forward control is possible by applying slow feedback control to the pump power.

Figure 4(a) shows the RF spectra of the feedback-controlled $f_{CEO/AOM}$ (in-loop) and f_{CEO} (out-of-loop). The servo bandwidth is estimated to be approximately 350 kHz from the bumps in the in-loop and out-of-loop spectra. The blue open circles in Fig. 4(b) show the RF spectrum of $f_{CEO/AOM}$ observed with feed-forward control during an evaluation operation (f_{CEO} ~ 10.7 MHz). Significant fringes appeared in the wings of the spectrum. These fringes mainly originated from the delay of the control signal traveling in the AOM medium. This delay is determined by the acoustic velocity in the medium and the distance between the optical path and the AOM transducer.[19] The blue solid curve in Fig. 4(b) shows the spectrum calculated using Eq. (6) in Ref. 20, assuming a delay time of 2.2 μs. The interference fringes appear with a period that is the inverse of the delay time, and the calculated spectrum fits well with the observed spectrum. Figure 4(c) shows the estimated noise suppression of the feed-forward-controlled $f_{CEO/AOM}$. The noise suppression falls to 0 dB at 110 kHz for a delay of 2.2 μs (blue solid curve) and the

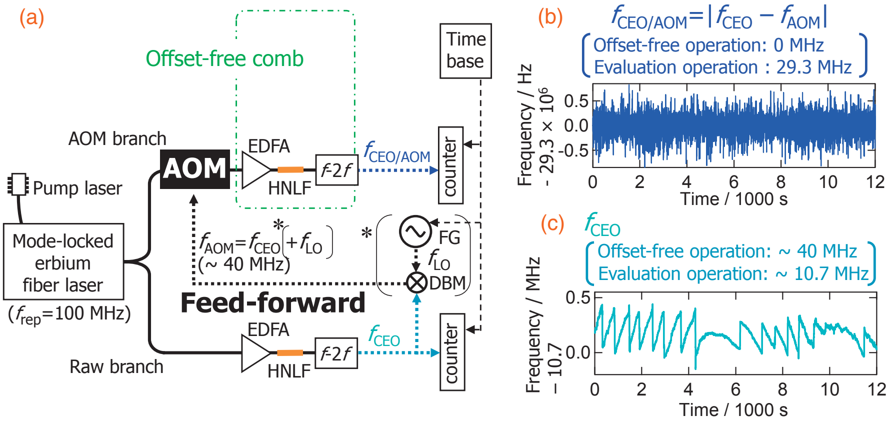

Fig. 3. (a) Experimental setup for “feed-forward” control. (b) $f_{\mathrm{CEO/AOM}}$ and (c) f_{CEO} counted during evaluation operation. *The FG and the DBM in the brackets were used only in the evaluation operation.

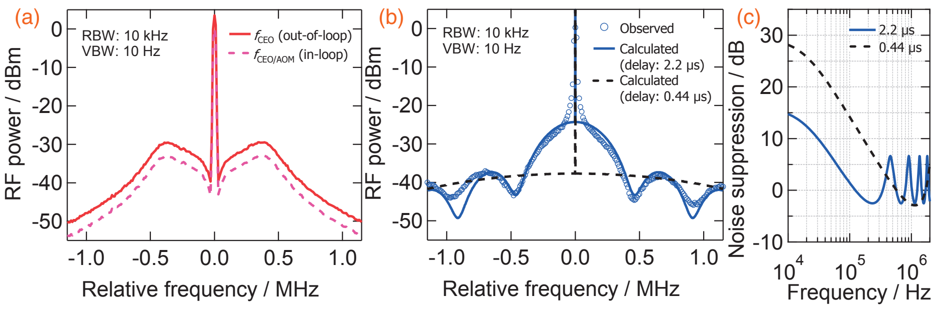

Fig. 4. (a) RF spectra of $f_{\mathrm{CEO/AOM}}$ (in-loop) stabilized with feedback control and f_{CEO} (out-of-loop). (b) RF spectra of $f_{\mathrm{CEO/AOM}}$ stabilized with feed-forward control. (c) Calculated noise suppression characteristics of feed-forward control.

frequency corresponds to the feed-forward control bandwidth. When the delay decreases to 0.44 µs, the S/N of the coherent peak of the feed-forward-controlled $f_{\mathrm{CEO/AOM}}$ is similar to that of the feedback-controlled f_{CEO}, as shown in Fig. 4(b) (black dashed curve). In this case, the noise suppression falls to 0 dB at 570 kHz, as shown in Fig. 4(c) (black dashed curve).

Figure 5 shows Allan deviations of the feedback-controlled $f_{\mathrm{CEO/AOM}}$ (in-loop), f_{CEO} (out-of-loop), and the feed-forward-controlled $f_{\mathrm{CEO/AOM}}$, which correspond to the frequency plots shown in Figs. 1(b), 1(c), and 3(b), respectively. The Allan deviations of the feedback-controlled f_{CEO} (out-of-loop) and the feed-forward-controlled $f_{\mathrm{CEO/AOM}}$ were, respectively, 0.10 and 0.18 Hz for a 1 s averaging time, and improved to 0.6 and 0.3 mHz for a 1000 s averaging time. With feedback stabilization, the Allan deviation of f_{CEO} (out-of-loop) was approximately 5 times higher than that of the $f_{\mathrm{CEO/AOM}}$ (in-loop) because the two branches were affected by different fiber noises induced by environmental disturbance. These results regarding the frequency instabilities are better than our previous results in terms of the relative frequency stability of a frequency comb including a CEO frequency[21] controlled by feedback without the use of any AOM (see black open diamonds in Fig. 5). This shows that the AOM has no negative impact on the frequency stability at this stability level. The frequency stability of the feedback- and feed-forward-controlled CEO frequencies is sufficiently high for many applications including frequency metrology.

In conclusion, we demonstrated an all-fiber-based offset-free frequency comb with a fiber-coupled AOM and two f–$2f$ interferometers using feedback or feed-forward control.

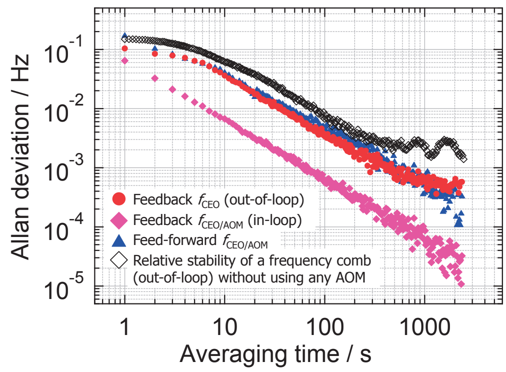

Fig. 5. Allan deviation of feedback-controlled $f_{\mathrm{CEO/AOM}}$ (in-loop) and f_{CEO} (out-of-loop), and feed-forward-controlled $f_{\mathrm{CEO/AOM}}$, which correspond to the frequency plots shown in Figs. 1(b), 1(c), and 3(b), respectively. The relative frequency stability of a frequency comb (out-of-loop) including a CEO frequency controlled by feedback without using any AOM is shown for comparison.

We observed the RF spectrum of the stabilized CEO beat under feed-forward control and found that it fitted our calculation well. We confirmed that both controls stabilize f_{CEO} at zero, and an offset-free comb can be realized using a second f–$2f$ interferometer. The all-fiber configuration using the fiber-coupled AOM provides a robust, cost-effective, and user-friendly offset-free comb with sufficiently high frequency stability for many applications, including ultrafast physics, frequency metrology, and optical communication.

Acknowledgment This work was supported by the Japan Science and Technology Agency (JST) through the ERATO MINOSHIMA Intelligent Optical Synthesizer (IOS) Project, Grant Number JPMJER1304.

1) D. J. Jones, S. A. Diddams, J. K. Ranka, A. Stentz, R. S. Windeler, J. L. Hall, and S. T. Cundiff, Science **288**, 635 (2000).
2) K. Iwakuni, S. Okubo, O. Tadanaga, H. Inaba, A. Onae, F.-L. Hong, and H. Sasada, Opt. Lett. **41**, 3980 (2016).
3) D. Nicolodi, B. Argence, W. Zhang, R. Le Targat, G. Santarelli, and Y. Le Coq, Nat. Photonics **8**, 219 (2014).
4) K. Minoshima and H. Matsumoto, Appl. Opt. **39**, 5512 (2000).
5) I. Coddington, W. C. Swann, and N. R. Newbury, Phys. Rev. Lett. **100**, 013902 (2008).
6) T. Steinmetz, T. Wilken, C. Araujo-Hauck, R. Holzwarth, T. W. Hansch, L. Pasquini, A. Manescau, S. D'Odorico, M. T. Murphy, T. Kentischer, W. Schmidt, and T. Udem, Science **321**, 1335 (2008).
7) S. Rausch, T. Binhammer, A. Harth, E. Schulz, M. Siege, and U. Morgner, Opt. Express **17**, 20282 (2009).
8) S. Koke, C. Grebing, H. Frei, A. Anderson, A. Assion, and G. Steinmeyer, Nat. Photonics **4**, 462 (2010).
9) S. Koke, A. Anderson, H. Frei, A. Assion, and G. Steinmeyer, Appl. Phys. B **104**, 799 (2011).
10) M. Yan, W. Li, K. Yang, H. Zhou, X. Shen, Q. Zhou, Q. Ru, D. Bai, and H. Zeng, Opt. Lett. **37**, 1511 (2012).
11) A. Baltuška, T. Fuji, and T. Kobayashi, Phys. Rev. Lett. **88**, 133901 (2002).
12) G. Krauss, D. Fehrenbacher, D. Brida, C. Riek, A. Sell, R. Huber, and A. Leitenstorfer, Opt. Express **36**, 540 (2011).
13) T. Nakamura, I. Ito, and Y. Kobayashi, Opt. Express **23**, 19376 (2015).
14) T.-H. Wu, K. Kieu, N. Peyghambarian, and R. J. Jones, Opt. Express **19**, 5313 (2011).
15) K. Tamura, H. A. Haus, and E. P. Ippen, Electron. Lett. **28**, 2226 (1992).
16) Y. Nakajima, H. Inaba, F. L. Hong, A. Onae, K. Minoshima, T. Kobayashi, M. Nakazawa, and H. Matsumoto, Opt. Commun. **281**, 4484 (2008).
17) T. R. Schibli, K. Minoshima, F. L. Hong, H. Inaba, A. Onae, H. Matsumoto, I. Hartl, and M. E. Fermann, Opt. Lett. **29**, 2467 (2004).
18) K. Iwakuni, H. Inaba, Y. Nakajima, T. Kobayashi, K. Hosaka, A. Onae, and F.-L. Hong, Opt. Express **20**, 13769 (2012).
19) M. Kourogi, B. Widiyatmoko, K. Imai, T. Shimizu, and M. Ohtsu, Opt. Lett. **24**, 16 (1999).
20) L. Richter, H. Mandelberg, M. Kruger, and P. McGrath, J. Quantum Electron. **22**, 2070 (1986).
21) Y. Nakajima, H. Inaba, K. Hosaka, K. Minoshima, A. Onae, M. Yasuda, T. Kohno, S. Kawato, T. Kobayashi, and T. Katsuyama, Opt. Express **18**, 1667 (2010).

